Epilepsy Research 154 (2019) 26–33

Contents lists available at ScienceDirect

Epilepsy Research

journal homepage: www.elsevier.com/locate/epilepsyres

Dexamethasone ameliorates the damage of hippocampal filamentous actin cytoskeleton but is not sufficient to cease epileptogenesis in pilocarpine induced epileptic mice

Nuo Yang[a,b], Yan-Chao Li[c], Tian-Qing Xiong[c], Ling-Meng Chen[c], Yu Zhai[d], Jian-Min Liang[a], Yun-Peng Hao[a], Di-Hui Ma[b,**], Yan-Feng Zhang[a,*]

[a] Department of Pediatric Neurology, The First Hospital of Jilin University, Changchun, Jilin Province 130021, PR China
[b] Department of Neurology, The First Hospital of Jilin University, Changchun, Jilin Province 130021, PR China
[c] Department of Histology and Embryology, College of Basic Medical Sciences, Norman Bethune Health Science Center of Jilin University, Jilin Province, 130021, PR China
[d] Department of Electrology, Chang Chun Children's Hospital, Changchun, Jilin Province 130000, PR China

ARTICLE INFO

Keywords:
Filamentous actin
Glucocorticoids
Dexamethasone
Epilepsy
Pilocarpine
Spontaneous seizures
Synapse maintenance

ABSTRACT

Rogressive deconstruction of filament actin (F-actin) in hippocampal neurons in the epileptic brain have been associated with epileptogenesis. Previous clinical studies suggest that glucocorticoids treatment plays beneficial roles in refractory epilepsy. Glucocorticoids treatment affects dendritic spine morphology by regulating local glucocorticoid receptors and F-actin cytoskeleton dynamics. However, how glucocorticoids regulate epileptogenesis by controlling F-actin cytoskeleton is not clear yet. Here we study the function of glucocorticoids in epileptogenesis by examining F-actin abundance, hippocampal neuron number, and synaptic markers in pilocarpine-induced epileptic mice in the presence or absence of dexamethasone (DEX) treatment. We found that spontaneous seizure duration was significantly reduced; F-actin damage in hippocampal subfields was remarkably attenuated; loss of pyramidal cells was dramatically decreased; more intact synaptic structures indicated by pre- and postsynaptic markers were preserved in multiple hippocampal regions after DEX treatment. However, the number of ZNT3 positive particles in the molecular layer in the hippocampus of pilocarpine epileptic mice was not altered after DEX treatment. Although not sufficient to cease epileptogenesis, our results suggest that dexamethasone treatment ameliorates the damage of epileptic brain by stabilizing F-actin cytoskeleton in the pilocarpine epileptic mice.

1. Introduction

Actin, a main component of both pre- and postsynaptic structures, exists in two states: as polymerized filaments (F-actin) or as monomers (G-actin) (Dillon and Goda, 2005). The dynamic regulation of cytoskeleton assembly and disassembly allows quick remodeling and balance between F- and G-actin in response to different neuronal activities (Dillon and Goda, 2005). Disturbance of the balance of actin assembly/disassembly and destabilized actin cytoskeleton, are observed in the epileptic brain and may contribute to the process of epileptogenesis. Acute seizures induced by kainate or 4-aminopyridine is accompanied by activation of cofilin, a actin-severing protein, and corresponding depolymerization of F-actin (Ouyang et al., 2007; Zeng et al., 2007). Our previous studies suggest that long-term remodeling of F-actin in hippocampal neurons occurs during chronic epileptic state in the pentylenetetrazole (PTZ) model and the pilocarpine-induced status epilepticus (SE) model (Xiong et al., 2015; Zhang et al., 2014a, b). Moreover, perfusion of latrunculin A, a drug causing F-actin-depolymerizing, results in an acute onset of epileptic seizures and chronic spontaneous seizures, associated with decreased seizure threshold and increased neuronal excitability (Sierra-Paredes et al., 2006). Interestingly, treatment of Ascomicin, or FK506, a pharmacological intervention antagonizing latrunculin A activity, decreases acute excitability of hippocampal neurons and ceases chronic seizures in epileptic models (Chwiej et al., 2010; Freire-Cobo et al., 2014; Xiong et al., 2018).

Glucocorticoids (GCs) as a clinical treatment have been used for many years for refractory epilepsies such as infantile spasm, Lennox–Gastaut syndrome, continuous spike-waves during slow-wave

* Corresponding author at: Department of Pediatric Neurology, The First Hospital of Jilin University, Changchun, Jilin Province 130021, PR China.
** Corresponding author at: Department of Neurology, The First Hospital of Jilin University, Changchun, Jilin Province 130021, PR China.
E-mail addresses: madihui916@126.com (D.-H. Ma), yfzhang@jlu.edu.cn (Y.-F. Zhang).

https://doi.org/10.1016/j.eplepsyres.2019.04.009
Received 11 October 2018; Received in revised form 2 January 2019; Accepted 17 April 2019
Available online 18 April 2019
0920-1211/

sleep (CSWS), variants of benign childhood epilepsy with centrotemporal spikes (BECT) and Landau-Kleffner Syndrome (LKS) (Buzatu et al., 2009; Chen et al., 2014; Hussain et al., 2014; Oftedal, 1967; Sinclair, 2003; Sinclair and Snyder, 2005; Tovia et al., 2011). Although glucocorticoids are widely used as a treatment of epilepsy, the underlying mechanism at molecular and cellular levels remain to be elucidated. Corticosterone, a glucocorticoid expressed in rodents, activates two types of receptors: high-affinity mineralocorticoid receptor (MR) and low-affinity glucocorticoid receptor (GR) (Tasker et al., 2006). Previous studies suggest that activation of MR exacerbate and GR ameliorate kainic acid (KA)-induced epilepsy by regulating synaptic plasiticity (Maggio and Segal, 2012). In the nervous system, GRs are localized to neuronal cell bodies, dendrites, as well as pre- and postsynaptic compartments and exert complex effects on synapse physiology and synaptic plasticity (Jafari et al., 2012; Johnson et al., 2005; Komatsuzaki et al., 2005; Krugers et al., 2010). Importantly, GRs regulate spine morphology and stability by controlling actin polymerization (Jafari et al., 2012). The dynamic change of actin network is the main driving force for both structural and functional plasticity of the synapse (Chazeau and Giannone, 2016). Thus, we wonder whether glucocorticoids ameliorate epilepsy by stabilizing synaptic structures and F-actin in spines.

Here, we examined the effect of dexamethasone (DEX), a potent GRs agonist, on the dynamic regulating of actin cytoskeleton in hippocampal neurons in a pilocarpine-induced epileptic mouse model. We observed changes in mice behavior and a reduction of neuronal cell loss in hippocampal regions. More stabilized F-actin and synaptic structures are observed after DEX treatment in pilocarpine epileptic mice. Our results provide the first evidence that GR activation regulates the epileptic brain by controlling actin dynamics in hippocampal neurons.

2. Material and methods

2.1. Pilocarpine induced epileptic model and group assignment

All the experiments were performed in adult male ICR mice weighing 22–24 g, obtained from Changsheng biotechnology (BX, China). Male were selected to avoid experimental differences due to gender. Mice were housed in groups and allowed free access to food and water in a quiet environment with a 12 h light and dark cycle at temperature of 22–26 ˚C. There were 3 days of acclimatization for animals before any experiment were performed. All pilocarpine models were induced between 8:00 am and 12:00 noon to reduce the impact of circadian on the epileptic susceptibility. Mice were intraperitoneally injected with 1 mg/kg methylscopolamine (Sigma-Aldrich, MO), followed by a single dose of 300 g/kg of pilocarpine (Sigma-Aldrich, MO, USA) 30 min later. After administration of pilocarpine, animal behaviors were monitored and seizures were evaluated by a modified version of the Racine scale (Racine, 1972; Shibley and Smith, 2002). Mice that developed a minimum of three stage 3–5 seizures episodes with continuous stage 1 and 2 seizures were considered to meet the standard of status epilepticus (SE) and received 4 mg/kg diazepam 2 h after onset. After SE induction, animals were supplied with moistened food in the cages to help replenish fluid. Mice that reached SE and survived were randomly divided into 2 groups: with or without DEX treatment, identified by PILO + DEX or PILO respectively. Mice in control group were age-matched male receiving scopolamine and saline injections. All the experimental procedures are approved by the Animal Research Committee of Jilin University. “Three Rs” were considered for our experimental design.

2.2. Drug administration

Our previous study suggests that three days following SE are critical for rearrangement of F-actin cytoskeleton (Xiong et al., 2015). This period following SE (depending on animal species, the dose of pilocarpine, and the duration of SE) is widely considered the latent period of pilocarpine model and is important for epileptogenetic process (Curia et al., 2008). Thus, in order to examine the effects of glucocorticoids in F-actin cytoskeletal remodeling during epileptogenesis we chose to administrate DEX at day 1–3 after SE. Between 9:00 and 10:00 AM on day 1, 2 and 3 after SE, 10 mg/Kg of dexamethasone (1702032, Suicheng Pharmaceutical Co., Ltd.) or an equal volume of saline was administered by intraperitoneal injection respectively.

2.3. Spontaneous seizure monitoring

Mice were monitored 2 h/day and 5 days/week between 9:00 − 11:00 AM to the day 28 after pilocarpine injection. The number of spontaneous recurrent seizures (SRS) was measured and the duration of each seizure was recorded. According to the Racine scale, seizures were divided into 5 stages. In this experiment, statistical analyses were performed in data sets where seizures that reached stage 4–5 of Racine scale.

2.4. Sample preparations

Samples were prepared as previously published studies (Zhang et al., 2014a, b). Briefly, 28 days after SE, mice were anesthetized with isoflurane, sacrificed, and subsequently perfused with 4% paraformaldehyde in 0.1 M PB. Brains were dissected out, post fixed, and immersed in a series of sucrose solutions with increased concentrations. Samples were frozen at -80℃ and sliced into thirty-micron-thick coronal sections on a Leica cryostat (GmbH, Germany) before experiments.

2.5. F-actin labeling

As described in previous studies (Zhang et al., 2014a, b), F-actin was labeled by the Alexa 488-conjugated phalloidin. After pretreatment with 0.3% Triton X-100 in 0.1 M phosphate buffer (pH 7.2) for 30 min, slices were incubated with Alexa 488-labeled phalloidin (1:100; A12379, Molecular Probes) at 4℃ overnight in the dark. After 3 washes, slices were mounted in anti-fade medium (Immu-Mount, Thermo Scientific, USA) and used for confocal imaging experiments.

2.6. Quantification of hippocampal neuron number

Anti-NeuN antibody was used to label the hippocampal neurons. Experimental procedures for anti-NeuN staining were described in previous studies (Xiong et al., 2018). Hippocampal slices were incubated with 10% normal donkey serum in 0.1 M PB containing 0.3% Triton X-100 for 30 min at room temperature and followed by monoclonal anti-NeuN antibody (1:100, ab177487, Abcam, USA) incubation at 4 ˚C overnight. Samples were then washed for three times in 0.1 M PB and were incubated in Alexa 488-labeled donkey anti-rabbit antibody (1:200, A21206, Molecular Probes) for 2 h at room temperature in the dark.

2.7. Postsynaptic marker PSD95 labeling

Slices were pretreated with pepsin to improve immunohistochemical detection of PSD95 (Fukaya and Watanabe, 2000). The experimental steps were described in our previous studies (Zhang et al., 2014a, b). After pepsin digestion, slices were incubated with 10% normal donkey serum in 0.1 M PB containing 0.3% Triton X-100 for 30 min at room temperature, with the primary antibody against PSD-95/SAP90 (1:100; No. 51-6900, Invitrogen, CA, USA) at 4 ˚C overnight, followed by incubation of Alexa 488 labeled donkey anti-rabbit IgG (1:200) for 2 h at room temperature in the dark.

2.8. Mossy Fiber terminals marker ZNT3 labeling

The mossy fiber synapses, enriched with zinc, have high release probabilities and exhibit synaptic plasticity expressed at presynaptic terminals. Standard immunocytochemistry was performed to label the hippocampal mossy fiber (MF) terminals. Primary antibody anti-ZNT3 (1:200; No. 197002, Synaptic Systems) and secondary antibody Alexa 546-conjugated donkey anti-rabbit IgG (1:200; Molecular Probes) were used. For double labeling of ZNT3 and F-actin, Alexa 488-conjugated phalloidin was co-incubated with the secondary antibody.

2.9. Image acquisition and data analysis

Fluorescence imaging of F-actin, NeuN, PSD95, ZNT3 was performed on an FV1000 confocal laser scanning microscope. Same experimental settings were used for each experiments. Detailed procedures were described in previous studies (Li et al., 2007; Zhang et al., 2014a). Hippocampal slices were randomly selected between the coordinates of anterior-posterior Bregma −1.28 to −2.12 mm. F-actin labeling density is measured using Image-Pro Plus analysis software (v. 6.0, Media Cybernetics, Silver Spring, MD). Fluorescence intensities of PSD95 and ZNT3 in different hippocampal subregions (see figure legends) were measured in Image *J* (National Institutes of Health, USA). At least in 3 fields for each subregion, and at least 3 sections were measured for each animal. The numbers of pyramidal cells in the hippocampal subregions CA1, CA3 and the dentate granule cells (DGCs) were counted as previously described (Wang et al., 2015; Xiong et al., 2018; Zhang et al., 2014a). Neurons in CA1 and CA3b and DGCs were counted in rectangular fields of a defined size in Image *J*. At least 3 sections were counted for each animal.

After a normality test with SPSS25 (IBM Corp., IBM SPSS Statistics Version 25.0, Armonk, NY, U.S.A), the original data were exported to GraphPad Prism 7 (GraphPad Software, Inc., La Jolla, CA, U.S.A.) for statistical analyses and figure preparations. Data subject to a normal distribution were presented as mean ± SD. Unpaired student *t*-test was performed in experiments with two conditions. One-way ANOVA with post hoc Turkey test was performed in experiments with three or more conditions. Data subject to an abnormal distribution were presented as M (P25, P75). The nonparametric statistics of Kolmogorov-Smirnov test was used for comparison between two groups and Kruskal-Wallis test was performed for three groups followed by a post hoc test of Dann's multiple comparison. The significance set for statistical analysis was $P < 0.05$.

3. Results

3.1. Pilocarpine-induced epileptic mice exhibit spontaneous seizures

After injection of pilocarpine, animals exhibited similar behavioral changes as previously reported (Xiong et al., 2015; Zhang et al., 2014b). Briefly, 64 in 73 mice (64/73) developed SE, including 29 mice (29/73) which died during or several hours after SE. The success and mortality rates were 47.94% and 39.73% respectively. No seizures and death were observed in the control group. All the animals used in the present study were summarized in Tables 1 and 2.

Behavioral change of mice was continuously monitored for 4 weeks after SE. we measured daily seizure numbers and recorded the duration of each seizure. Three days after SE, spontaneous recurrent seizures (SRS) were observed successively in pilocarpine induced mice. All the animals survived from SE developed SRS of stage IV or V in the following 24 days (including 5 dead during the following experiments). Compared with the PILO group, DEX administration decreased the duration of SRS (Fig. 1B), but the number of SRS onset was similar to that of group without DEX treatment (Fig. 1A).

Table 1
The number of mice used in this experiment.

Mice that did not develop SE		9
Mice that died during or immediately after SE		29
Mice that developed SE	Mice that died during the experiments	5
	PILO	15
	PILO + DEX	15
Control		15
Total		88

Table 2
The experimental design of each group.

	Control	PILO	PILO + DEX
SRS observations	n = 15	n = 15	n = 15
F-actin detection	n = 7	n = 7	n = 7
Anti-Neun			
Anti-PSD95			
Anti-ZNT3			
Anti-ZNT3/F-actin			

3.2. Dexamethasone treatment attenuates F-actin damage in hippocampal neurons

The abundance of F-actin in hippocampal subregions was examined by phalloidin staining. In the control group, F-actin displayed large clustered puncta in CA3 stratum lucidum (SL) (Fig. 2 A and A1) and hilus of dentate gyrus (DG) (Fig. 2 G and G1), but displayed tiny evenly distributed puncta in CA1 stratum radiation (SR) (Fig. 2 D and D1). The fluorescence density of F-actin immunolabeling was remarkably decreased in different regions in hippocampus in the PILO-injected group (Fig. 2 B-B1 for CA3; E-E1 for CA1; H and H1 for the hilus of DG) compared to the control group (Fig. 2 A-A1 for CA3; D-D1 for CA1; G and G1 for hilus of DG). After treatment with DEX, decrease of F-actin in hippocampal subfields of PILO-injected mice was dramatically reduced as shown in Fig. 2 (Fig. 2 C-C1 for CA3; F-F1 for CA1; I and I1 for hilus of DG). Statistical analysis of F-actin density showed that DEX treatment ameliorated the decrease of F-actin in hippocampal subfields of the CA3 (Fig. 2J), CA1 (Fig. 2K) and hilus of DG (Fig. 2L) in PILO-injected animals.

3.3. Dexthamethason treatment reduces pyramidal neuron loss in CA1 and CA3 but does not change DGCs proliferation

We then performed anti-NeuN staining to examine whether DEX treatment had protective effects on the SE-induced neuron damage. We observed a remarkable pyramidal cell loss in CA1 and CA3 regions in the hippocampus in PILO-injected group (Fig. 3 D and E) compared to the control group (Fig. 3A and B). We also observed an increase of DGC number in PILO-injected group compared to control animals(Fig. 3F). Although DEX treatment didn't completely rescue the neuronal loss induced by SE, the number of remaining NeuN-positive cells increased in the CA1 and CA3 regions in the DEX treatment group (Fig. 3 G and H). Consistently, statistical analysis showed that DEX treatment significantly reduced the loss of neurons in both CA1 and CA3 subfields (Fig. 3J and K). However, DEX treatment did not show any effect on DGCs proliferation (Fig. 3I and 3 L).

3.4. DEX treatment alters synaptic remodeling in hippocampal subfields

We then tested whether DEX treatment affect neuronal function at the synapse level. We examined synapse morphology and abundance by examining pre-/post-synaptic markers in epilepsy models. Postsynaptic PSD95 abundance, quantified by measuring fluorescence intensity, was severely decreased in PILO-injected group (Fig. 4 D for CA3; E for CA1; F for hilus of DG), compared to control group (Fig. 4 A for CA3; B for CA1; C for hilus of DG). After DEX treatment, the decrease in PSD95

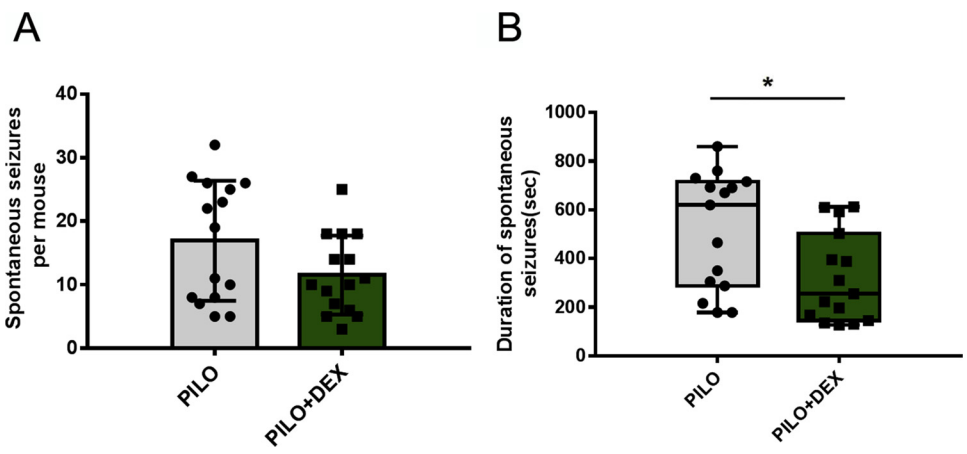

Fig. 1. Effects of DEX treatment on spontaneous seizures onset.
Number (A) and duration (B) of SRS per mouse in different groups are shown respectively. Compared to PILO group, DEX administration reduced the duration of SRS (B), but the number of SRS was similar to that of group without DEX treatment (A). (n = 15 per group; *, $p < 0.05$)

intensity was effectively prevented in different hippocampal subfields (Fig. 4 G for CA3; H for CA1; I hilus of DG). Statistical analysis of PSD95 fluorescence intensity showed that DEX treatment ameliorated the SE-induced reduction of PSD95 in CA3 (Fig. 4J), CA1 (Fig. 4K) and hilus of DG (Fig. 4L) in the hippocampus.

Large mossy fiber terminals (LMTs) of DGCs, is among the most powerful presynaptic terminals in the brain. We also examined whether there were any changes at the synapse level at LMT terminals. LMTs, indicated by the positive granules of ZNT3, were distributed from the hilus of DG to the SL of CA3 in control group, and no positive granules were observed in the molecular layer (ML) of DG (Fig. 5 A1 and D1). We found the fluorescence intensity of ZNT3 was dramatically decreased in the PILO-injected animals compared to control group (Fig. 5 B1and E1). However, positive particles were observed in the ML of the

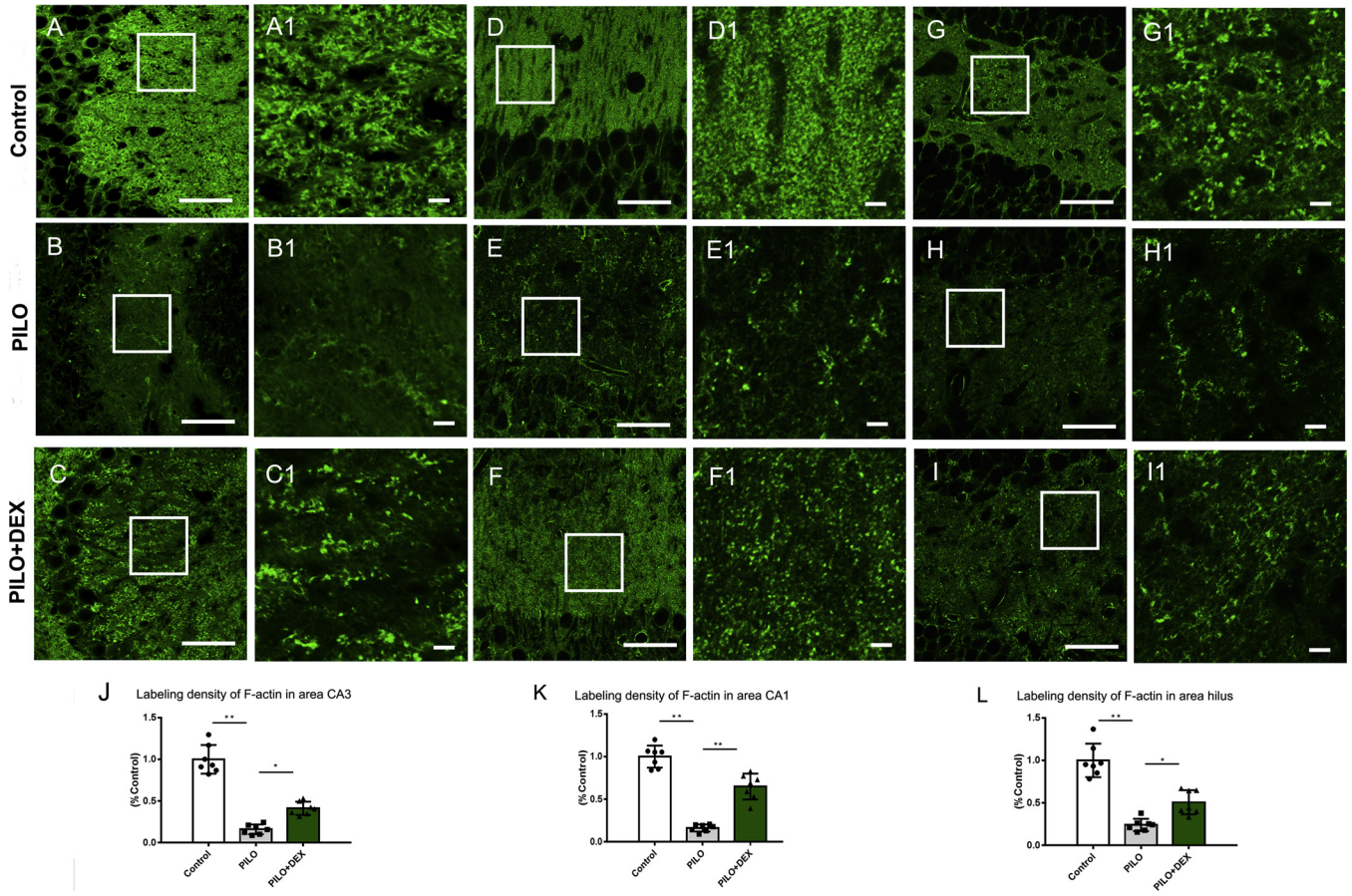

Fig. 2. DEX treatment attenuates the damage of hippocampal F-actin.
Distribution of F-actin in subregions of CA3 stratum lucidum, CA1 stratum radiatum and the hilus of DG is shown in A—C, D-F and G—I respectively. A1–I1 are images with higher magnifications for A–I. In the control group, F-actin displays large clustered puncta in the subfields of CA3 stratum lucidum (A and A1), hilus of DG (G and G1), and tiny, evenly distributed puncta in the subregion of CA1 stratum radiation (D and D1). As compared to the control group, F-actin density is remarkably decreased in the PILO group (B-B1 for CA3; E-E1 for CA1; H and H1 for the hilus of DG). After treatment of DEX, the decrease of F-actin in hippocampal subfields of PILO mice is partially rescued as shown (C-C1 for CA3; F-F1 for CA1; I and I1 for hilus of DG). Statistical analysis of labeling density of F-actin shows that DEX treatment ameliorates the decrease of F-actin in hippocampal subfields of the CA3 (*J*), CA1 (K) and hilus of DG (L). (n = 7 per group; *, $P < 0.05$; **, $P < 0.001$). Scale bars: A—I, 50 μm; A1–I1, 5 μm.

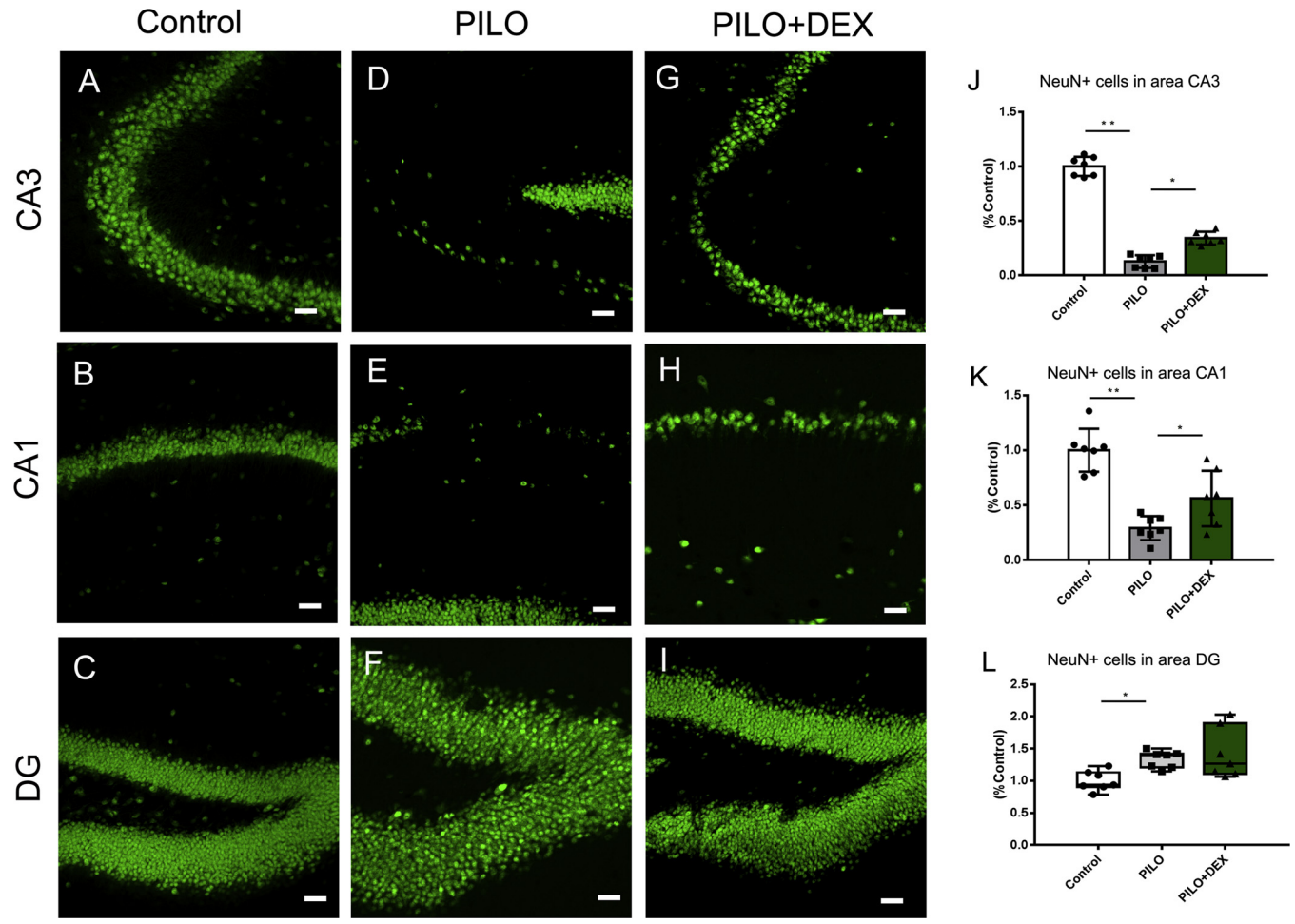

Fig. 3. DEX treatment reduces pyramidal neurons loss in subfields CA1 and CA3, but does not change the proliferation of DGCs.
Relative to the saline controls (A and B), the pyramidal cells in the subfields CA1 and CA3 are lost remarkably in PILO mice (D and E). After treatment of DEX (G and H), the number of Neu**N**-positive cells in subfields CA1 and CA3 is increased. Statistical analysis shows that DEX treatment remarkably reduces the loss of neurons in both subfields (*J* and K). However, DEX treatment does not show any effect on the proliferation of DGCs. In the subfield DG, the number of DGCs increases remarkably in both PILO and PILO + DEX groups (F and I). Statistical analysis shows that DEX treatment does not attenuate the proliferation of DGCs (L). (n = 7 per group ; *, P < 0.05; **, P < 0.001). Scale bars: 50 μm.

PILO group (Fig. 5 E1, white arrows). DEX treatment rescued the decrease of ZNT3-positive terminals in hippocampal subfields (Fig. 5C1 and F1). However, ZNT3-positive particles in the ML were still observed in the DEX-treated mice (Fig. 5 F1, white arrows). Statistical analysis of fluorescence intensity of ZNT3 showed that DEX treatment attenuated the decrease of ZNT3 remarkably in subfields CA3 (Fig. 5H), and hilus of DG (Fig. 5I).

Double fluorescence labeling of phalloidin and ZNT3 was performed to examine the relationship of F-actin and LMTs in different experimental groups. In the PILO-injected mice, ZNT3-positive puncta decreased in the SL of CA3 where F-actin intensity was also reduced correspondingly (Fig.5B1-B3). In the DEX-treated group, ZNT3 reduction was significantly attenuated with the relative reduction of F-actin in the SL of subfield CA3 (Fig. 5C1-C3). However, some ZNT3-positive puncta appeared in the in the ML of DG and these newly-appearing ZNT3 puncta were located in close proximity to F-actin puncta in the molecular layer. The colocalization of ZNT3 and F-action were shown in image with high (Fig. 5G). These results suggest that although DEX treatment partially rescue F-action damage, it does not change LMT synapse remodeling.

4. Discussion

Cumulative studies seek for the molecular mechanisms of glucocorticoids in the treatment of epilepsy, but it is still not clear how glucocorticoids regulate epileptogenesis at the molecular and synapse levels. For example, dexamethasone showed effects on seizures reduction (Al-Shorbagy et al., 2012; Pieretti et al., 1992; Yilmaz et al., 2014), anti-Inflammation (Borham et al., 2016; Marchi et al., 2011; Vizuete et al., 2018) neuron protection (Al-Shorbagy et al., 2012), and anti-astrogliosis (Vizuete et al., 2018). Clinical studies also provide evidence that glucocorticoids treatment reduce seizures onset and improve cognition in patients with refractory epilepsy (Buzatu et al., 2009; Chen et al., 2014; Hussain et al., 2014; Oftedal, 1967; Sinclair, 2003; Sinclair and Snyder, 2005; Tovia et al., 2011). However, previous studies also suggest seizures and brain injuries were exacerbated with dexamethasone treatment (Duffy et al., 2014; Lee et al., 1989). These discrepancies might be caused by different time-points, durations and dosages of glucocorticoids administration. Differential effects of three dosages of DEX were evaluated in a lithium-pilocarpine induced epileptic model. DEX at the dose of 10 mg/kg showed an effect of anticonvulsion, while neither 5 mg/kg nor 20 mg/kg played protective roles in this study (Al-Shorbagy et al., 2012). Consistently, in a penicillin induced epileptic model, the effects of DEX administration on epileptiform activity at dosages of 1, 3, and 10 mg/kg were examined respectively. DEX remarkably decreased spike frequencies at 3 mg/kg and 10 mg/kg. However, it is worth noting that administration of DEX at 3 mg/kg increases epileptiform activity at early stage (10–40 minutes

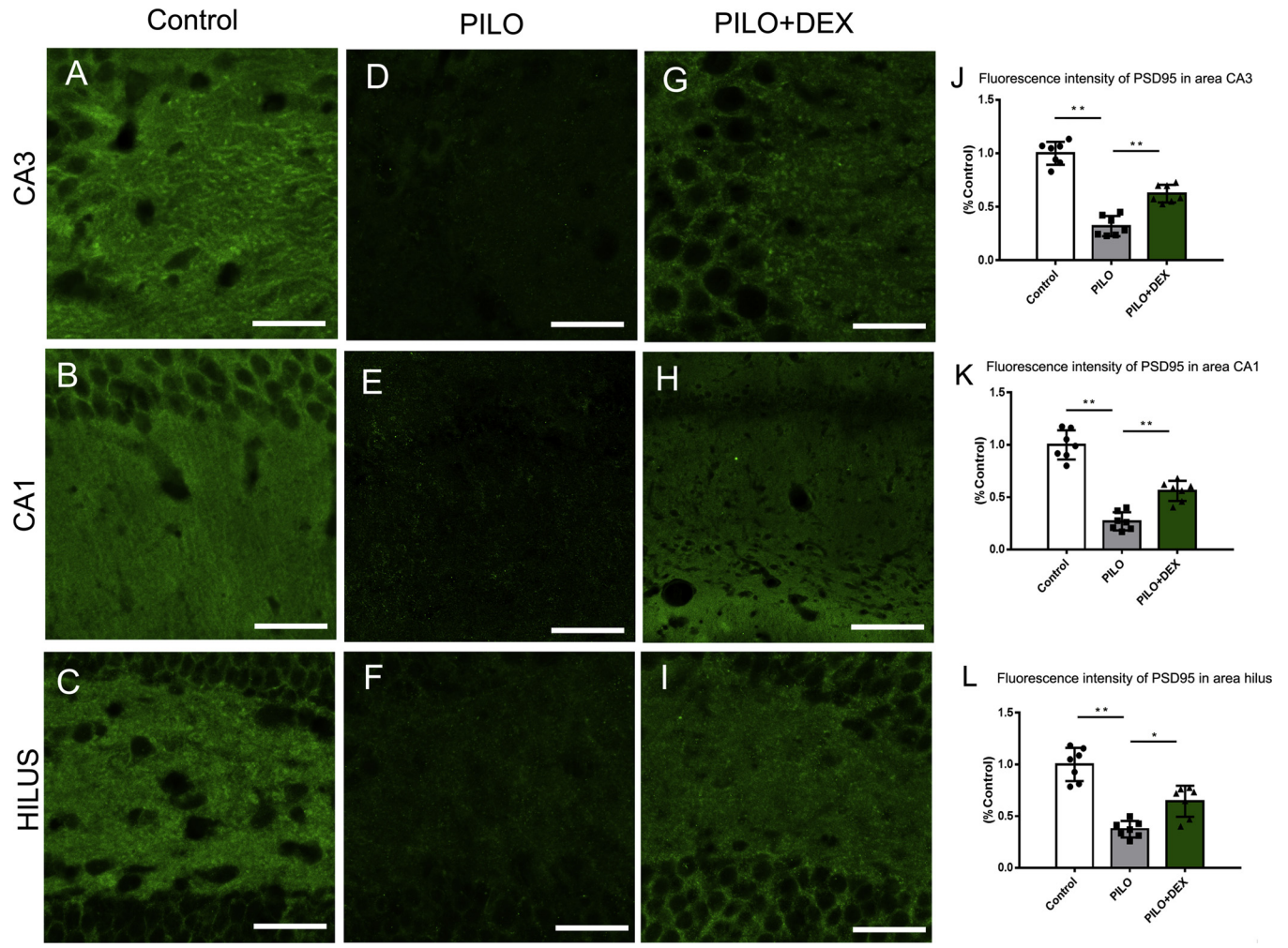

Fig. 4. DEX treatment reduces the decrease of PSD95 in hippocampus. Compared with the control group (A for CA3; B for CA1; C for hilus of DG), PSD95 fluorescence intensity is dramatically decreased in the PILO group (D for CA3; E for CA1; F for hilus of DG). With treatment of DEX, the reduction of PSD95 fluorescence intensity is effectively prevented in hippocampal subfields (G for CA3; H for CA1; I hilus of DG). Statistical analysis of fluorescence intensity of PSD95 shows that DEX treatment attenuates the SE-induced decrease of PSD95 in hippocampal subfields of the CA3 (*J*), CA1 (K) and hilus of DG (L). (n = 7 per group ; *, $P < 0.05$; **, $P < 0.001$). Scale bars: 50 μm.

after injection), indicating a time-dependent effect of DEX treatment (Yilmaz et al., 2014). In line with previous findings, our present study showed that administration of three doses of DEX at 10 mg/kg displayed a positive effect on the treatment of epilepsy.

Here, we injected DEX 3 days following SE, and focused on its chronic effect on the rearrangement of F-actin cytoskeleton, neuronal loss and synaptic remodeling. The mechanisms involved in this process remain largely unknown. Both GR/MR function, and genomic/non-genomic actions may play important roles. Receptors of glucocorticoids in the brain have been identified for about fifty years and there are two kinds of glucocorticoids receptors in the brain, high affinity MR and low affinity GR. High doses of glucocorticoids activate GRs and low doses activate MRs. Interestingly, these two types of glucocorticoids receptors play opposite roles in many different cellular processes (Joels, 2006, 2018). The counteractive activities of MRs and GRs may provide an explanation for the dose-dependent effects of glucocorticoids in the treatment of epilepsy. Thus, we speculate in the case of present studies that administration of 3 doses of 10 mg/kg DEX activate GRs in the epilepsy models.

Moreover, transcriptional regulation of gene expression caused by glucocorticoid may also affect actin cytoskeleton dynamics. It is reported previously that glucocorticoids remodel actin cytoskeleton in various cell types in a protein synthesis-dependent manner (Castellino et al., 1992, 1995; Mayanagi et al., 2008). In contract, glucocoritcoids induced non-transcriptional regulation can also affect actin polymerization (Stournaras et al., 2014). Exposure to DEX triggered a rapid polymerization of F-actin, reduced the ratio of G-actin and stabilized the filamentous structures (Koukouritaki et al., 1996). Further evidence suggests that the effects on reorganization of actin cytoskeleton were related to non-transcriptional regulation of actin network (Koukouritaki et al., 1997). GRs are localized in dendritic spines and are important for regulating the actin network through G protein coupled pathways. Administration of DEX, an agonist of GRs, induces a rapid increase of the cofilin phosphorylation and activates extracellular signal-regulated kinase (ERK) ½, and thereby stabilizes actin cytoskeleton in dendritic spines. This effect can be blocked by RU-486, an antagonist of GRs (Jafari et al., 2012). Based on the data above, we speculate that DEX might activate GRs on dendritic spines, to promote the actin polymerization and to stabilize filamentous structures in our studies.

The effect of DEX on cell survival in different hippocampal regions in epilepsy was also examined in our current studies. We showed that DEX treatment attenuated the loss of pyramidal cells in subfields CA1 and CA3. The relationship between F-actin damage and loss of neuron in pilocarpine model had been reported in our previous studies (Xiong et al., 2015, 2018; Zhang et al., 2014b). The two events co-occur at similar time-points and brain regions. F-actin depolymerization occurs

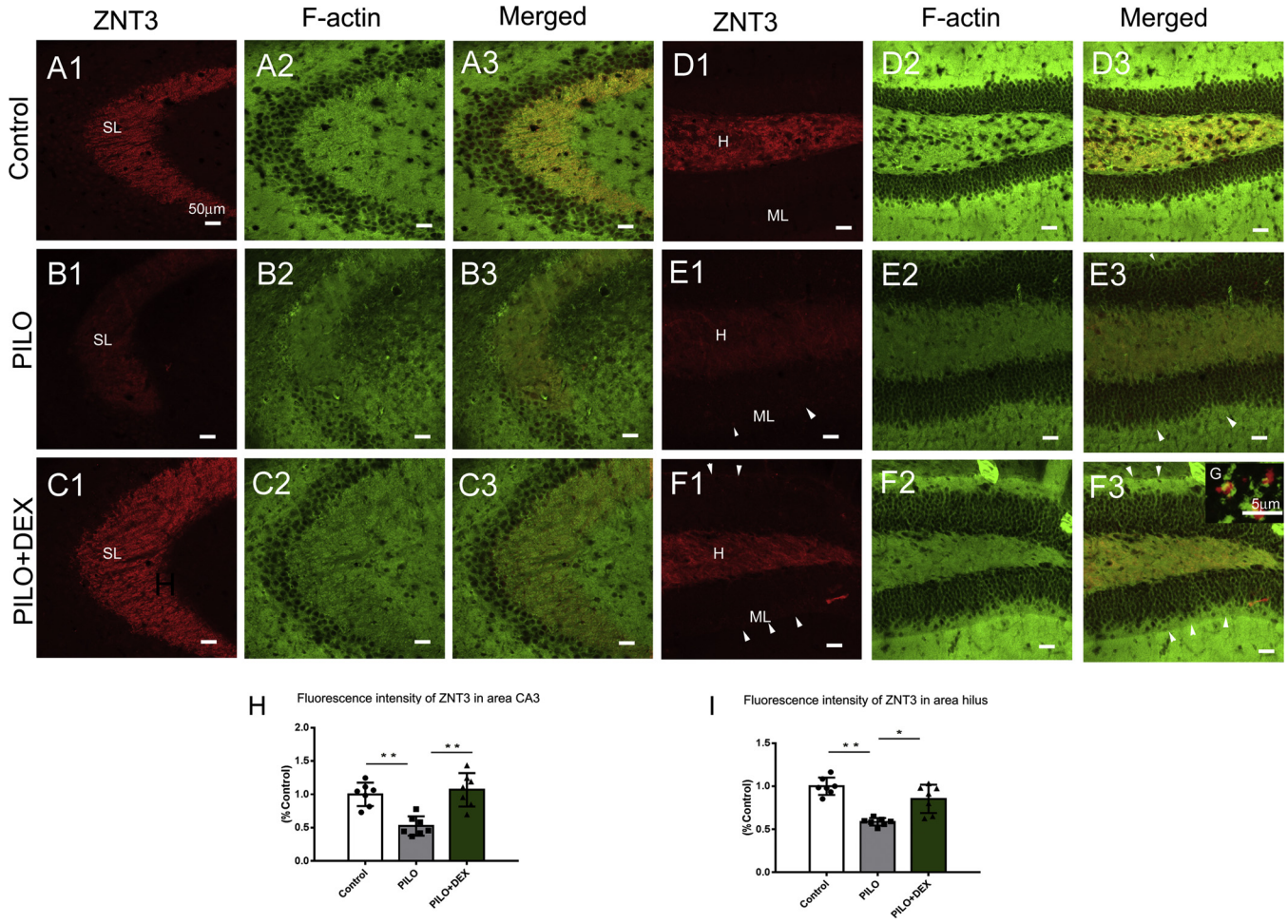

Fig. 5. Effect of DEX treatment on ZNT3 in hippocampal subfields.
Representative images A1–C1, D1–F1 (red) show ZNT3 granules in the subfields of CA3 SL, hilus and molecular layer (ML) of DG in different groups. Images A2–C2, D2–F2 (green) show F-actin puncta in the same regions. Images A3 - F3 are merged from A1–F1 and A2–F2 respectively. G is partially magnified from F3 arrow area. In the controls (A1 and D1), the positive granules of ZNT3 are distributed from the hilus of DG to the SL of area CA3. No positive granules are observed in the ML of DG. As compared to the controls, the fluorescence intensity of ZNT3 is dramatically reduced (B1and E1) in the areas where F-actin intensity is decreased (B1-B3, E1-E3) and some positive particles appear in the ML in the PILO group (E1, **white** arrows). DEX treatment reverts the decrease of ZNT3 to a great extent in hippocampal subfields (C1 and F1) in PILO mice. However, ZNT3 positive particles in the ML of are still observed in the DEX-treated PILO mice (F1, **white** arrows). Statistical analysis of fluorescence intensity of ZNT3 shows that DEX treatment nearly reverses the decrease of ZNT3 in subfield CA3 (H), and recovers it in subfield hilus of DG (H). The enlarged imagine (G) show puncta of F-actin and ZNT3 are located in close proximity (yellow) indicating their **co**-localization. (n = 7 per group ; *, $P < 0.05$; **, $P < 0.001$); (SL, stratum lucidum; ML, molecular layer ; H, hilus of DG). Scale bars : A1–F3, 50 μm; G, 5 μm.

during cell death in various cell models (Guenal et al., 1997; Korichneva and Hammerling, 1999; Kruidering et al., 1998; Song et al., 2013). Thus the preservation of neurons after DEX treatment may contribute to the less damage of F-actin in the present study. However, there is also evidence suggesting that the actin cytoskeleton plays a key role in the communication network to decide the death or survival of cells (Korichneva and Hammerling, 1999). Stabilization of actin cytoskeleton improves the survival potential to apoptosis, while destabilization of actin cytoskeleton abets cells to death (Korichneva and Hammerling, 1999). Correspondingly, F-actin depolymerization was accompanied by the loss of hippocampal neurons in the pilocarpine induced epileptic mice (Xiong et al., 2015; Zhang et al., 2014b). Thus, we also propose a model that DEX treatment preserve F-actin structure and thereby protect neurons from cell death during epilepsy.

Considering that the actin cytoskeleton is located in both pre- and post- synapse, we further examined pre-/post- synaptic markers to examine the effects of glucocorticoids on synaptic remodeling in epileptic models. Consistent with the changes of F-actin, the damage of PSD95, the post-synaptic marker, was significantly alleviated in area CA1, CA3, and hilus in DEX treatment group. The presynaptic marker, ZNT3, also showed a corresponding change in area CA3 and hilus. Modulation of synapses under glucocorticoid administration has been reported previously. Application of glucocorticoid rapidly increases the density of thorny excrescences of pyramidal neurons in CA3 subfield through activating synaptic GRs and the following kinase pathways (Komatsuzaki et al., 2012). Consistent with these findings, our studies showed relatively more preserved pre- and post- synaptic structures after DEX treatment in pilocarpine induced epileptic mice. The fact that more F-actin structures remained in the hippocampus after DEX treatment contributes this results to the critical role of F-actin stabilization in synaptic remodeling (Chazeau and Giannone, 2016; Dillon and Goda, 2005). However, the mossy fiber terminals, labeled with ZNT3, showed significant proliferation in the molecular layer in both the pilocarpine and the DEX treatment groups. The newly generated presynaptic terminals have formed complex connections with F-actin on the day28, indicating a long term synaptic remodeling in this brain area. Mossy fiber sprouting and aberrant recurrent circuits made the function of DG as a high resistance gate compromised, allowing the invasion of epileptiform activity from the entorhinal cortex to the hippocampus (Koyama, 2016).

5. Conclusions

Taken together, we examined the remodeling of actin dynamics in the epileptic brain after glucocorticoid treatment. It showed that administration of 10 mg/Kg DEX 3 days following SE ameliorates the damage of hippocampal filamentous actin cytoskeleton, alleviates the loss of hippocampal neurons and contributes to the maintenance of synaptic structures, but is not sufficient to cease epileptogenesis.

Acknowledgements

Yanfeng Zhang and Dihui Ma make the equal contribution to the present study. This study is funded by National Natural Science Foundation of China (Number: 81401068; 81801284) and Department of Science and Technology of Jilin Province of China (Number: 20180101159JC).

References

Al-Shorbagy, M.Y., El Sayeh, B.M., Abdallah, D.M., 2012. Diverse effects of variant doses of dexamethasone in lithium-pilocarpine induced seizures in rats. Can. J. Physiol. Pharmacol. 90, 13–21.

Borham, L.E., Mahfoz, A.M., Ibrahim, I.A.A., Shahzad, N., ALrefai, A.A., Labib, A.A., Bin Sef, B., Alshareef, A., Khan, M., Milibary, A., Al Ghamdi, S., 2016. The effect of some immunomodulatory and anti-inflammatory drugs on Li-pilocarpine-induced epileptic disorders in Wistar rats. Brain Res. 1648, 418–424.

Buzatu, M., Bulteau, C., Altuzarra, C., Dulac, O., Van Bogaert, P., 2009. Corticosteroids as treatment of epileptic syndromes with continuous spike-waves during slow-wave sleep. Epilepsia 50 (Suppl. 7), 68–72.

Castellino, F., Heuser, J., Marchetti, S., Bruno, B., Luini, A., 1992. Glucocorticoid stabilization of actin filaments: a possible mechanism for inhibition of corticotropin release. Proc. Natl. Acad. Sci. U S A 89, 3775–3779.

Castellino, F., Ono, S., Matsumura, F., Luini, A., 1995. Essential role of caldesmon in the actin filament reorganization induced by glucocorticoids. J. Cell Biol. 131, 1223–1230.

Chazeau, A., Giannone, G., 2016. Organization and dynamics of the actin cytoskeleton during dendritic spine morphological remodeling. Cell. Mol. Life Sci. 73, 3053–3073.

Chen, J., Yang, Z., Liu, X., Ji, T., Fu, N., Wu, Y., Xiong, H., Wang, S., Chang, X., Zhang, Y., Bao, X., Jiang, Y., Qin, J., 2014. Efficacy of methylprednisolone therapy for electrical status epilepticus during sleep in children. Zhonghua Er Ke Za Zhi 52, 678–682.

Chwiej, J., Janeczko, K., Marciszko, M., Czyzycki, M., Rickers, K., Setkowicz, Z., 2010. Neuroprotective action of FK-506 (tacrolimus) after seizures induced with pilocarpine: quantitative and topographic elemental analysis of brain tissue. J. Biol. Inorg. Chem. 15, 283–289.

Curia, G., Longo, D., Biagini, G., Jones, R.S., Avoli, M., 2008. The pilocarpine model of temporal lobe epilepsy. J. Neurosci. Methods 172, 143–157.

Dillon, C., Goda, Y., 2005. The actin cytoskeleton: integrating form and function at the synapse. Annu. Rev. Neurosci. 28, 25–55.

Duffy, B.A., Chun, K.P., Ma, D., Lythgoe, M.F., Scott, R.C., 2014. Dexamethasone exacerbates cerebral edema and brain injury following lithium-pilocarpine induced status epilepticus. Neurobiol. Dis. 63, 229–236.

Freire-Cobo, C., Sierra-Paredes, G., Freire, M., Sierra-Marcuno, G., 2014. The calcineurin inhibitor Ascomicin interferes with the early stage of the epileptogenic process induced by Latrunculin A microperfusion in rat hippocampus. J. Neuroimmune Pharmacol. 9, 654–667.

Fukaya, M., Watanabe, M., 2000. Improved immunohistochemical detection of postsynaptically located PSD-95/SAP90 protein family by protease section pretreatment: a study in the adult mouse brain. J. Comp. Neurol. 426, 572–586.

Guenal, I., Risler, Y., Mignotte, B., 1997. Down-regulation of actin genes precedes microfilament network disruption and actin cleavage during p53-mediated apoptosis. J. Cell. Sci. 110 (Pt 4), 489–495.

Hussain, S.A., Shinnar, S., Kwong, G., Lerner, J.T., Matsumoto, J.H., Wu, J.Y., Shields, W.D., Sankar, R., 2014. Treatment of infantile spasms with very high dose prednisolone before high dose adrenocorticotropic hormone. Epilepsia 55, 103–107.

Jafari, M., Seese, R.R., Babayan, A.H., Gall, C.M., Lauterborn, J.C., 2012. Glucocorticoid receptors are localized to dendritic spines and influence local actin signaling. Mol. Neurobiol. 46, 304–315.

Joels, M., 2006. Corticosteroid effects in the brain: U-shape it. Trends Pharmacol. Sci. 27, 244–250.

Joels, M., 2018. Corticosteroids and the brain. J. Endocrinol. 238, R121–R130.

Johnson, L.R., Farb, C., Morrison, J.H., McEwen, B.S., LeDoux, J.E., 2005. Localization of glucocorticoid receptors at postsynaptic membranes in the lateral amygdala. Neuroscience 136, 289–299.

Komatsuzaki, Y., Murakami, G., Tsurugizawa, T., Mukai, H., Tanabe, N., Mitsuhashi, K., Kawata, M., Kimoto, T., Ooishi, Y., Kawato, S., 2005. Rapid spinogenesis of pyramidal neurons induced by activation of glucocorticoid receptors in adult male rat hippocampus. Biochem. Biophys. Res. Commun. 335, 1002–1007.

Komatsuzaki, Y., Hatanaka, Y., Murakami, G., Mukai, H., Hojo, Y., Saito, M., Kimoto, T., Kawato, S., 2012. Corticosterone induces rapid spinogenesis via synaptic glucocorticoid receptors and kinase networks in hippocampus. PLoS One 7, e34124.

Korichneva, I., Hammerling, U., 1999. F-actin as a functional target for retro-retinoids: a potential role in anhydroretinol-triggered cell death. J. Cell. Sci. 112 (Pt 15), 2521–2528.

Koukouritaki, S.B., Theodoropoulos, P.A., Margioris, A.N., Gravanis, A., Stournaras, C., 1996. Dexamethasone alters rapidly actin polymerization dynamics in human endometrial cells: evidence for nongenomic actions involving cAMP turnover. J. Cell. Biochem. 62, 251–261.

Koukouritaki, S.B., Margioris, A.N., Gravanis, A., Hartig, R., Stournaras, C., 1997. Dexamethasone induces rapid actin assembly in human endometrial cells without affecting its synthesis. J. Cell. Biochem. 65, 492–500.

Koyama, R., 2016. Dentate circuitry as a model to study epileptogenesis. Biol. Pharm. Bull. 39, 891–896.

Krugers, H.J., Hoogenraad, C.C., Groc, L., 2010. Stress hormones and AMPA receptor trafficking in synaptic plasticity and memory. Nat. Rev. Neurosci. 11, 675–681.

Kruidering, M., van de Water, B., Zhan, Y., Baelde, J.J., Heer, E., Mulder, G.J., Stevens, J.L., Nagelkerke, J.F., 1998. Cisplatin effects on F-actin and matrix proteins precede renal tubular cell detachment and apoptosis in vitro. Cell Death Differ. 5, 601–614.

Lee, P.H., Grimes, L., Hong, J.S., 1989. Glucocorticoids potentiate kainic acid-induced seizures and wet dog shakes. Brain Res. 480, 322–325.

Li, Y.C., Bai, W.Z., Hashikawa, T., 2007. Regionally varying F-actin network in the apical cytoplasm of ependymocytes. Neurosci. Res. 57, 522–530.

Maggio, N., Segal, M., 2012. Stress and corticosteroid modulation of seizures and synaptic inhibition in the hippocampus. Exp. Neurol. 234, 200–207.

Marchi, N., Granata, T., Freri, E., Ciusani, E., Ragona, F., Puvenna, V., Teng, Q., Alexopolous, A., Janigro, D., 2011. Efficacy of anti-inflammatory therapy in a model of acute seizures and in a population of pediatric drug resistant epileptics. PLoS One 6, e18200.

Mayanagi, T., Morita, T., Hayashi, K., Fukumoto, K., Sobue, K., 2008. Glucocorticoid receptor-mediated expression of caldesmon regulates cell migration via the reorganization of the actin cytoskeleton. J. Biol. Chem. 283, 31183–31196.

Oftedal, S.I., 1967. Steroid treatment of infantile spasms with hypsarrhythmia. Electroencephalogr. Clin. Neurophysiol. 23, 390–391.

Ouyang, Y., Yang, X.F., Hu, X.Y., Erbayat-Altay, E., Zeng, L.H., Lee, J.M., Wong, M., 2007. Hippocampal seizures cause depolymerization of filamentous actin in neurons independent of acute morphological changes. Brain Res. 1143, 238–246.

Pieretti, S., Di Giannuario, A., Loizzo, A., Sagratella, S., Scotti de Carolis, A., Capasso, A., Sorrentino, L., 1992. Dexamethasone prevents epileptiform activity induced by morphine in in vivo and in vitro experiments. J. Pharmacol. Exp. Ther. 263, 830–839.

Racine, R.J., 1972. Modification of seizure activity by electrical stimulation. II. Motor seizure. Electroencephalogr. Clin. Neurophysiol. 32, 281–294.

Shibley, H., Smith, B.N., 2002. Pilocarpine-induced status epilepticus results in mossy fiber sprouting and spontaneous seizures in C57BL/6 and CD-1 mice. Epilepsy Res. 49, 109–120.

Sierra-Paredes, G., Oreiro-Garcia, T., Nunez-Rodriguez, A., Vazquez-Lopez, A., Sierra-Marcuno, G., 2006. Seizures induced by in vivo latrunculin a and jasplakinolide microperfusion in the rat hippocampus. J. Mol. Neurosci. 28, 151–160.

Sinclair, D.B., 2003. Prednisone therapy in pediatric epilepsy. Pediatr. Neurol. 28, 194–198.

Sinclair, D.B., Snyder, T.J., 2005. Corticosteroids for the treatment of Landau-kleffner syndrome and continuous spike-wave discharge during sleep. Pediatr. Neurol. 32, 300–306.

Song, Y., Hou, J., Qiao, B., Li, Y., Xu, Y., Duan, M., Guan, Z., Zhang, M., Sun, L., 2013. Street rabies virus causes dendritic injury and F-actin depolymerization in the hippocampus. J. Gen. Virol. 94, 276–283.

Stournaras, C., Gravanis, A., Margioris, A.N., Lang, F., 2014. The actin cytoskeleton in rapid steroid hormone actions. Cytoskeleton Hoboken (Hoboken) 71, 285–293.

Tasker, J.G., Di, S., Malcher-Lopes, R., 2006. Minireview: rapid glucocorticoid signaling via membrane-associated receptors. Endocrinology 147, 5549–5556.

Tovia, E., Goldberg-Stern, H., Ben Zeev, B., Heyman, E., Watemberg, N., Fattal-Valevski, A., Kramer, U., 2011. The prevalence of atypical presentations and comorbidities of benign childhood epilepsy with centrotemporal spikes. Epilepsia 52, 1483–1488.

Vizuete, A.F.K., Hansen, F., Negri, E., Leite, M.C., de Oliveira, D.L., Goncalves, C.A., 2018. Effects of dexamethasone on the Li-pilocarpine model of epilepsy: protection against hippocampal inflammation and astrogliosis. J. Neuroinflammation 15, 68.

Wang, N., Mi, X., Gao, B., Gu, J., Wang, W., Zhang, Y., Wang, X., 2015. Minocycline inhibits brain inflammation and attenuates spontaneous recurrent seizures following pilocarpine-induced status epilepticus. Neuroscience 287, 144–156.

Xiong, T., Liu, J., Dai, G., Hou, Y., Tan, B., Zhang, Y., Li, S., Song, Y., Liu, H., Li, Y., Li, Y., 2015. The progressive changes of filamentous actin cytoskeleton in the hippocampal neurons after pilocarpine-induced status epilepticus. Epilepsy Res. 118, 55–67.

Xiong, T.Q., Chen, L.M., Tan, B.H., Guo, C.Y., Li, Y.N., Zhang, Y.F., Li, S.L., Zhao, H., Li, Y.C., 2018. The effects of calcineurin inhibitor FK506 on actin cytoskeleton, neuronal survival and glial reactions after pilocarpine-induced status epilepticus in mice. Epilepsy Res. 140, 138–147.

Yilmaz, T., Akca, M., Turan, Y., Ocak, H., Kamasak, K., Yildirim, M., 2014. Efficacy of dexamethasone on penicillin-induced epileptiform activity in rats: an electrophysiological study. Brain Res. 1554, 67–72.

Zeng, L.H., Xu, L., Rensing, N.R., Sinatra, P.M., Rothman, S.M., Wong, M., 2007. Kainate seizures cause acute dendritic injury and actin depolymerization in vivo. J. Neurosci. 27, 11604–11613.

Zhang, Y.F., Li, S.L., Xiong, T.Q., Yang, L.B., Li, Y.N., Tan, B.H., Liu, Q., Li, Y.C., 2014a. The rearrangement of filamentous actin in mossy fiber synapses in pentylenetetrazol-kindled C57BL/6 mice. Epilepsy Res. 108, 20–28.

Zhang, Y.F., Xiong, T.Q., Tan, B.H., Song, Y., Li, S.L., Yang, L.B., Li, Y.C., 2014b. Pilocarpine-induced epilepsy is associated with actin cytoskeleton reorganization in the mossy fiber-CA3 synapses. Epilepsy Res. 108, 379–389.